RESEARCH PAPER

Dielectric behaviour of emeraldine base polymer–ZnO nanocomposite film in the low to medium frequency

M. L. Singla · Rajeev Sehrawat · Nidhi Rana · Kulvir Singh

Abstract Emeraldine base (EB) polymer–ZnO nanoparticles composite films has been synthesized by solution casting technique on ITO-coated glass substrate and characterized by XRD, FTIR and TEM for their structure and morphology. Dielectric behaviour of these composite films has been investigated in the very low frequency region to medium frequency region (1 kHz–1 MHz). The dielectric constant of the composite with 30% nanoparticles is almost one-tenth of the pure EB. The dielectric value becomes constant in the frequency region greater than 400 kHz. The change in dielectric behaviour of the composite is explained on the basis of multilayered interface formed between the ZnO nanoparticles and emeraldine chains. Nanoparticles have high energy surface which is responsible for the decrease of free volume for the orientation of polymer chains consequently decrease in dielectric constant of the composite. TEM images shows about 10 nm ZnO particles embedded in the emeraldine matrix. From the XRD data it has been observed that the lattice parameters of ZnO have been modified due to the alignment of polymer chains along the basal planes of the nanoparticles. The shift of N=Q=N and N–B–N vibration bands to higher wave number in IR indicates that interaction between emeraldine chain and nanoparticles which provides stability to emeraldine matrix.

Keywords Nanocomposite · Polymer · Interface · Dielectric · XRD · Synthesis · Nanoparticles

M. L. Singla (✉) · R. Sehrawat · N. Rana
Central Scientific Instruments Organisation (CSIR, New Delhi), Sector 30, Chandigarh 160030, India
e-mail: singla_min@yahoo.co.in

K. Singh
Thapar University, Patiala 147001, Punjab, India

Introduction

Polyaniline (PANI) is environmentally stable and highly tuneable conducting polymer, which can be produced as bulk powder, cast films, or fibres (MacDiarmid and Epstein 1989). Polymeric chain consists of a succession of reduced benzenic nucleus and oxidised quinoidic nucleus. Both insulating emeraldine base (EB) and conducting emerladine salt (ES) are the stable forms. (Cao et al 1992; MacDiarmid and Epstein 1994). ZnO is semiconducting in nature having unique properties like large exciton binding energy (60 meV) and relatively large direct band gap of ~ 3.3 eV at room temperature (Andeen et al 2003; Chen et al 1998). Advantage associated with these properties includes higher breakdown voltages, ability to sustain large electric fields, low electric noise and high temperature and high power operations (Ozgur et al. 2005). It has been studied extensively for making optical and electronic

devices like: light emitting diodes, solar cells, transducers, varistors, photo detectors, etc., (Saito et al. 2002; Koch et al 1995; Liang et al 2001). The incorporation of nanoparticles into the polymer offers enhanced performance for both the host and the guest. The polymer nanocomposites are promising candidates based on the fact that the small-sized particles enhance the properties while the polymer matrix offers flexible functionalities to control host–guest interaction to ensure the growth and distribution of nanoparticles (Gangopadhyay 2000). Hence by choosing particular choice of the matrix and the filler particles, one can modify the properties of the composite for a particular application.

Some study has been done on the bulk PANI–ZnO composites for its dielectric behaviour in microwave region (Sharma et al 2009). As nanoparticles have large surface to volume ratio, they lead to change the properties as compared to the bulk material. Hence, the incorporation of the ZnO nanoparticles in the EB form may lead to certain different results as compared to the bulk particles.

However to the best of our knowledge no study has been reported on dielectric behaviour of EB–ZnO nano-composite in this frequency region (1 kHz–1 MHz). The dielectric properties of such a material are much relevant for telecommunication applications in aerospace and for EMI shielding. A low and stable dielectric constant is often desirable for application such as high-speed integrated package and satellite communication. In this paper we report synthesis of PANI–ZnO nanocomposite films and their dielectric behaviour in the frequency range (1 kHz–1 MHz).

Experimental

Materials and synthesis

High purity zinc acetate dihydrate (98%), hydrochloric acid (35% GR), ammonium peroxidisulphate (98%), methanol (99.8%), aniline (99.5%), *N*-methyl-2-pyrolidone (NMP) (99%), and ammonia (30% GR) were purchased from Merck & Co., Inc., and were used as received. Distilled water was employed as a medium to polymerize aniline.

EB was synthesized by chemical oxidative polymerization method (Stejskal 2002). In a typical

experiment to polymerize aniline, 5 ml of aniline monomer was mixed with 100 ml of 2 M HCl solution in a glass beaker. The mixture was continuously stirred for half an hour at 0 °C. 8.0 g ammonium peroxidisulphate was dissolved in water by its minimum quantity to prepare a solution, which is then added drop-wise to the above mixture with constant stirring. The colour of the reaction mixture changed to dark green. This solution was kept for overnight. The solution was filtered in a Buchrer funnel and the residue obtained was washed several times with distilled water till no acid remained. To make PANI soluble in organic solvent, the residue was treated with 10% ammonia solution to form PANI EB form . The solution and precipitates turned blue. The precipitates were filtered, washed with distilled water and the residue was dried in oven at 60 °C for 5 h. It was grounded with a mortar and pestle, sieved through 20-μm sieve and stored in a glass container. It is an insulating form.

ZnO nanoparticles was synthesised as described earlier (Seow et al. 2009). In a typical experiment, zinc acetate dihydrate (3.35 mmol) was first dissolved in methanol (31.25 ml) and another solution of potassium hydroxide (6.59 mmol) was prepared by dissolving it into methanol (16.25 ml). The potassium hydroxide solution was added drop-wise to the zinc acetate solution at 60 °C under vigorous stirring. After 1.5 h, nanoparticles started to precipitate and the solution became turbid. The heating and stirring were discontinued after 2 h and the solution was allowed to stand for another 2 h. The ZnO nanoparticles settled at the bottom and the excess mother liquor was removed. Precipitates were washed twice with methanol (12.5 ml). A portion of precipitate was dispersed in a mixture of 12.5 ml of methanol and 2.5 ml of chloroform for TEM imaging. The dispersed solution was translucent and stable for about 2 weeks**.** The other portion of precipitate was air dried and stored as ZnO nanoparticles.

Growth of films

The known amount of EB powder (1 g) was dissolved in NMP (10 ml). The solution was stirred for 4 h to make EB completely soluble. This solution was filtered using a Whatman filter paper having pore size of 6 μm to get clear solution. A film of this solution was deposited by solution casting technique

on the ITO-coated glass substrates. These films were allowed to dry at room temperature for 72 h.

For the EB–ZnO nanocomposites film (10%), ZnO nanoparticles (0.01 gm) were dispersed in 1 ml of EB solution in NMP (containing 0.1 g EB). Similarly, 20 and 30% ZnO nanoparticles were dispersed in EB–NMP solution. Each solution was stirred for 5 h continuously. The films from these composites solutions were prepared on an ITO-coated glass substrate by the solution casting technique. These films were allowed to dry at room temperature for 72 h. All characterisations and dielectric behaviour were studied using film specimens having uniform thickness of 5.0 ± 0.02 μm.

Characterisation techniques

The thickness of EB as well as composite films was measured with the help of a mechanical profilometer (From Talysurf Series 2 Instrument). X-ray diffraction studies were carried out using **a** PANalytical's X'Pert PRO X-ray diffractometer system in 2θ range of 20–80°. XRD patterns were analyzed by matching the observed peaks with the standard pattern provided by the JCPDS file. The lattice parameters for ZnO were calculated for nanoparticles and for composite. EB and EB–ZnO (20 wt%) composite was studied in the frequency range of 500–2000 cm^{-1} by Fourier Transform Infra Red (FTIR) spectroscope (Model: Perkin Elmer RX-1). A transmission electron microscopy (TEM model: Hitachi H7600) was used to investigate the dispersion of ZnO particles in EB. Dielectric measurements of films of EB and EB–ZnO composites were carried out by Network analyzer (model: HIOKI3532-50 LCR HiTESTER) in the frequency range of 1 kHz–1 MHz. Figure 1 shows the schematic presentation of the measurement of the dielectric constant.
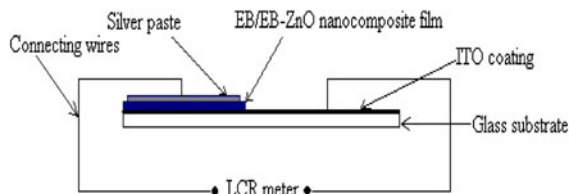
To measure the dielectric properties, one half area of the glass substrate was coated with EB or composites and another half was uncoated to form a capacitor. Conducting silver paste was used to form the electrodes in contact with coated and uncoated side. Silver-based conducting paste is widely used. They have reasonably high conductivity and provide good contact to the materials (in this case polymer films). Silver paste is not directly soldered and conduction relies on point to point contact between polymer film and ITO surface. Moreover, polymer composite as a whole is a neutral species therefore it does not react with silver paste. Similar configuration has been reported in literature (Harsányi 1995). The dielectric constant (ε_r) of each film was calculated using the equation:
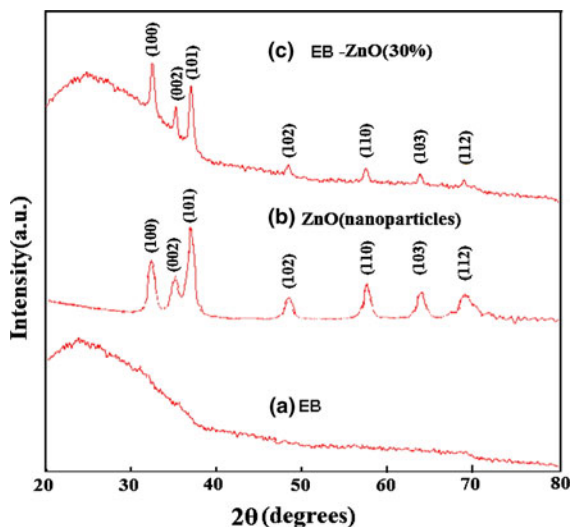
$$C = \varepsilon_r \varepsilon_o \, a/d$$

Where ε_o is the vacuum permittivity, which equals 8.85×10^{-12} F/m, a is the electrode area and d is the thickness of film.

Results and discussion

Structure and morphology

The XRD patterns of EB, ZnO nano-crystal and EB-ZnO (30%) composite films are as shown in Fig. 2. The XRD pattern of EB is in conformation with the earlier reported results as only a broad peak was observed at $2\theta = 23°$ (Fig. 2a) showing the amorphous nature (Pouget et al. 1991).

Figure 2b shows the powder XRD patterns of the ZnO nanoparticles synthesized at 60 °C after its solution casting on the glass substrate. The XRD patterns of as obtained ZnO nanoparticles are of hexagonal wurzite structure. The characteristic peaks are observed at 31.720, 34.500, 36.300, 47.760, 56.60, 63.100 and 68.000 which corresponds to miller indices (100) (002) (101) (102) (110) (103) and (201), respectively. The lattice constants are obtained as $a = b = 3.2269$ Å and $c = 5.2539$ Å using powder XRD software. All the diffraction peaks are in agreement with JCPDS data (card no. 36-1451, $a = b = 3.249$ Å, $c = 5.206$ Å). The results indicate that product consist of pure phase and no characteristic peaks for other impurity like Zn(OH)$_2$. The sharp peak indicates that the nanoparticles are

Fig. 1 Schematic diagram used for the dielectric constant measurement of EB and EB–ZnO nanocomposite films on ITO coated glass

Fig. 2 XRD pattern for (*a*) EB powder, (*b*) ZnO nanoparticles film grown over ITO-coated glass and (*c*) EB-ZnO (30%) nanocomposite film over ITO coated glass

well crystallized. The small particles size makes the diffraction peaks broader than corresponding standard pattern. In contrast to the standard card, the (002) peak is stronger, revealing the (001) oriented growth of ZnO nanoparticles.

ZnO has a hexagonal closed-packed wurtzite structure having alternating planes of Zn and O atoms. The (002) plane is parallel to the planes which are containing O and Zn atoms while the (100) plane is perpendicular to the (002) plane, intersecting alternating layers of Zn and O atoms. The crystalline size in (002) and (100) plane can be essentially considered as matrices of diameter (D) and length (L), respectively.

The crystallite size of ZnO was found to be $\sim 9.5 \pm 0.5$ nm as calculated from the first three prominent peaks using the Scherrer formula ($L = 0.93\ \lambda/\beta\cos\theta$), where L is the average crystallite size, λ is the wave length of Cu (1.54 Å), β is the full width of diffraction line at half the maximum intensity and θ is the Bragg angle.

The XRD of the composite (Fig. 2c) has similar pattern as that of ZnO powder; however the peak intensity was modified. ZnO has retained its hcp wurtzite structure in the composite. The presence of XRD peak of emeraldine at 2θ value of 23° with lower intensity indicates the dilution of the EB concentration due to adsorption of EB chains on nanoparticle surface. From the XRD peaks, it was

observed that lattice parameter for nanocomposite were $a = b = 3.2442$ Å, $c = 5.2061$ Å. This change of lattice parameter of ZnO nanoparticle on formation of composite with EB shows that the unit cell of ZnO stretches along horizontal direction and suppresses along c-axis. This might be attributed due to higher surface along the prism plane as compared to the basal plane in hexagonal close packed crystal structure. Similar results have been reported (Sharma et al 2009) for PANI–ZnO composites. The stretching of unit cell in a–b plane and suppression along c-axis suggests strong interaction between ZnO nanoparticles surface with the EB molecular chains. The crystallite size calculated from the first three major peaks found to be $\sim 11.5 \pm 0.5$ nm.

The typical TEM images of as prepared ZnO nanostructure is given in Fig. 3. It is clear from the image that the spherical nanoparticles are mono dispersed with size 5–9 nm ranges and maximum particles are of 6 nm size. TEM images of EB-ZnO nanocomposite in Fig. 4 clearly shows entrapping of ZnO nanoparticles in emeraldine matrix. Moreover, the nanoparticles still remain monodispersive with
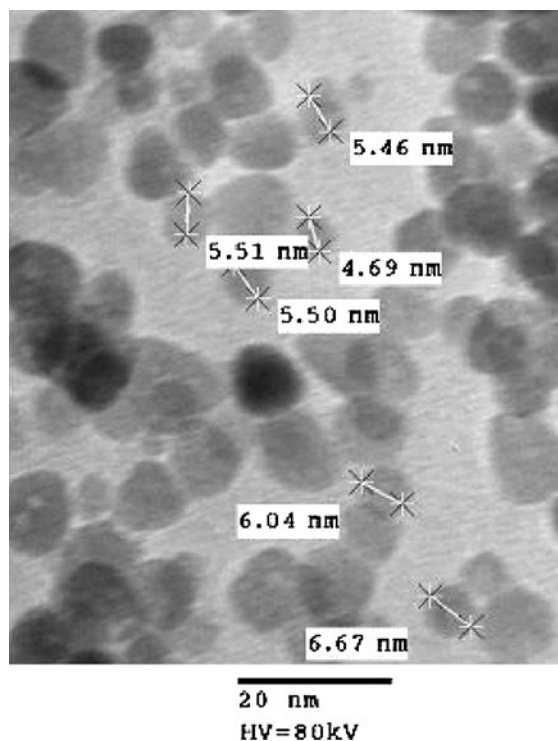
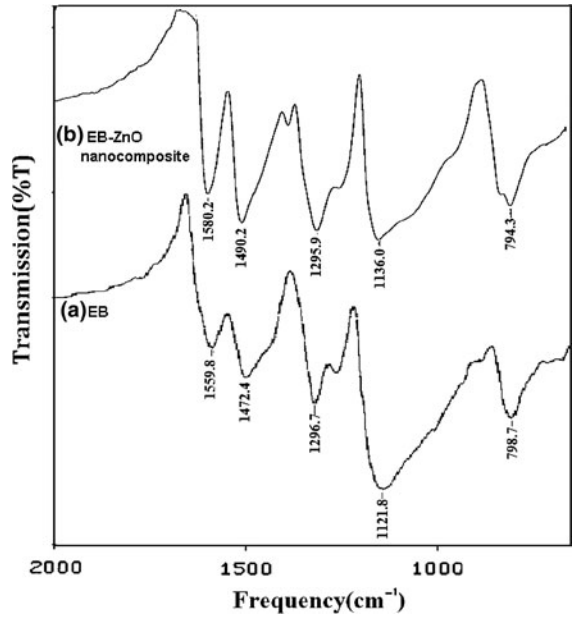**Fig. 3** Typical TEM image of the synthesised ZnO nanoparticles
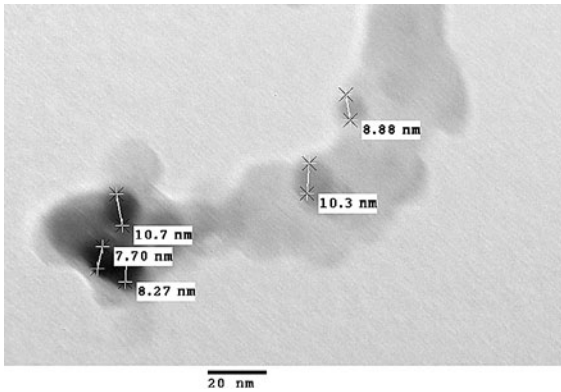
Fig. 4 Typical TEM of EB–ZnO (30%) nanocomposite

Fig. 5 FTIR spectra of (*a*) EB, (*b*) EB–ZnO (30%) nanocomposite

average diameter around 10 nm. The increase in the size of nanoparticles in the nanocomposite indicates that the surface of nanoparticle has interaction with EB chains, which is also clear from FTIR analysis. Similarly, XRD analysis also shows the increase in size of ZnO nanoparticles in the composite. XRD average nanoparticle size is somewhat larger in comparison to TEM image, because for XRD analysis nano-powder was prepared by air drying the synthesized particles. There is a possibility of agglomeration as no surfactant has been used for capping during synthesis. Moreover, TEM image gives the size of the individual nanoparticle, whereas the size calculated from the XRD patterns represents average size.

FTIR

FTIR spectra of pure EB and EB–ZnO (30%) nanocomposite in KBr are shown in the Fig. 5. The characteristics peaks of PANI at 798.7, 1121.8, 1296.7, 1472.4 and 1559.8 cm^{-1} corresponds to the C–H out of plane, C–H in plane bending, C–N stretching vibration of secondary amine, stretching mode of the N–B–N benzoid rings, stretching mode of the N=Q=N quinoid rings, respectively (Tan et al. 2009; Zeng and Ko 1997). The nanocomposite also shows the similar characteristic peaks. But the corresponding peaks of pure EB have been shifted to 794.3, 1136.0, 1296.9, 1490.2, and 1580.2 cm^{-1} in nanocomposite. The shift may be described due to the formation of hydrogen bonding on the surface of ZnO nanoparticles and –NH– group of EB. Similar interaction has been also reported earlier (He 2005; Paul et al 2007).

Dielectric behaviour

Variation of dielectric constant (ε_r) of EB and nanocomposite films as a function of frequency (1 kHz–1 MHz) is shown in Fig. 6. The dielectric constant of EB film decreases from 76.19 to 67.63 in
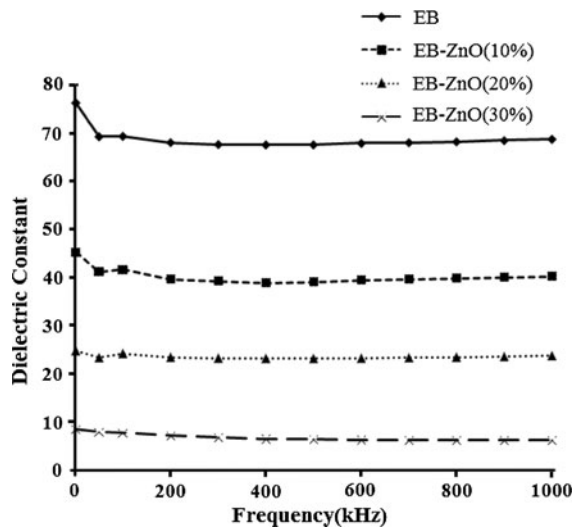
Fig. 6 Variation of dielectric constant in frequency range of 1 kHz-1 MHz for. (*a*) EB, (*b*) EB–ZnO (10%) nanocomposite, (*c*) EB–ZnO (20%) nanocomposite, (*d*) EB–ZnO (30%) nanocomposite

the frequency range 1–400 kHz and then increase to 68.27 in frequency range upto 1 MHz. For nanocomposite with 10% ZnO nanoparticles ε_r decreases from 45.2 to 39.7 in the frequency range 1–400 kHz and then again increases to 41.43. For nanocomposite with 20% ZnO nanoparticles, composite ε_r decreases from 24.86 to 23.31 in 1–500 kHz frequency range and then changes minutely to the value 23.87 upto 1 MHz frequency, indicating that with increase of nanoparticle concentration in the nanocomposite, the values ε_r is lowered and then tends to be saturated. However, nanocomposite with 30% ZnO nanoparticles, ε_r decrease from 8.57 to 6.56 in the frequency range 1 to 400 kHz. There is no further variation in the values of ε_r. The dielectric constant becomes constant in the frequency range 400 kHz–1 MHz which is important for many technological applications. The value of ε_r for the nanocomposite with 10% ZnO, 20% ZnO and 30% ZnO decrease by a factor ~ 2, ~ 3 and ~ 9, respectively, in comparison to pure EB. Average measurement values of dielectric constant w.r.t. frequency (for ten observations) of each sample along with error bars are given in Table 1. The variation in the measured values of the dielectric constant ranges from ± 0.02 to ± 0.05.

The decrease in dielectric constant value with variation in concentration of ZnO nanoparticles in the nanocomposite can be explained on the basis of lower dielectric constant of ZnO than EB and multi-layered core model (Tanaka and Kozako 2005). The dielectric constant of ZnO has been reported in the range of 7.5–10 depending on processing conditions

(Crisler et al 1968). The lower dielectric constant of 30% ZnO contained nanocomposite might be attributed due to low value of ZnO nanoparticles and their distribution in polymeric matrix (Dang et al 2003, Huang 2010). Multilayered core model accounts for the filler particles which are spherical in nature. Thus, this model has applied in present studies as synthesized ZnO nanoparticles are nearly spherical in shape as observed from TEM images and the ZnO nanoparticles are stable in EB matrix as indicated by XRD study. According to this model, the interface between inorganic (ZnO) filler nanoparticles and polymer EB matrix contain three different layers: (a) bonded layer, (b) bounded layer and (c) loose layer.

The first layer (bonded layer) is due to the hydrogen bonding between the ZnO nanoparticles and the EB chains which is a thin molecular transition layer. The second interfacial layer (bounded layer) is formed as other EB chains are strongly bound or interacted to the first layer and ZnO nanoparticles. This interaction has been explained on the basis of the defects present in the ZnO structure. In nanostructured ZnO, the small length scales and large surface-to-volume ratio mean that surface defects play a stronger role in controlling properties. The dominant defects which occur in ZnO structure is the oxygen vacancies and Zn-interstitials (Hagemark 1976). These defects donate two electrons resulting in over all negative charge on the ZnO structure. Due to these defects, the EB chains interact strongly with ZnO nanoparticles. The third layer is formed due to the loose interaction of the EB chains with second layer. This interaction

Table 1 Average measurement values of dielectric constant w.r.t. frequency (for ten observations) of each nanocomposite sample along with error bars

Frequency (kHz)	EB $\pm$ 0.05	EB–ZnO (10%) $\pm$ 0.05	EB–ZnO (20%) $\pm$ 0.04	EB–ZnO (30%) $\pm$ 0.02
1	76.19	45.32	24.86	8.57
50	69.29	41.21	23.47	8.02
100	69.37	41.67	24.32	7.88
200	68.11	39.67	23.58	7.28
300	67.71	39.36	23.39	6.78
400	67.63	38.95	23.33	6.56
500	67.64	39.12	23.31	6.41
600	67.94	39.47	23.37	6.37
700	68.08	39.79	23.46	6.31
800	68.27	39.91	23.58	6.29
900	68.51	40.02	23.72	6.29
1000	68.77	40.24	23.87	6.28

leads to the change in chain conformation, chain mobility, crystallinity, and free volume of the loose layer as compared to the polymer matrix.

The reduction in permittivity has been explained by the contribution from both, bounded and loose layer.

Role of bounded layer:

The dielectric constant of the EB is due to the orientation polarization (Joseph Mathai et al. 2002). In the presence of electric field, the strongly polarizable bond (C=N) tend to orient in the direction of the field. However, this orientation of polar group is a slow process, but in lower frequency range (1 kHz–1 MHz) there is sufficient time for the complete orientation of the polar bond in the field direction. Thus this polarization may get completed in this frequency region. The dielectric constant of the EB is due to the strongly polarizable C=N bond in conjugated polymer chain. EB chains interact with polar ZnO nanoparticles in inner bounded layer in the presence of electric field. The polarity of ZnO impair the motion of the C=N dipoles resulting in decrease of dielectric constant.

Role of loose layer

The second layer is formed due to interaction of EB chains with oxygen defects present on the surface ZnO nanoparticles. As the ZnO nanoparticles have high surface energy, thus interaction becomes stronger in second layer. However, further adsorption /diffusion of EB polymer chains with second layer becomes weak resulting in reduced free volume. It has already been discussed that free volume in polymer-filler composite system decreases in nanostructure composite materials and increases in microstructure composite materials (Nelson and Hu 2004). This reduction in free volume explains the reduction in permittivity (Bal and Kothari 2009). With the increase of ZnO nanoparticle concentration in the composite, the dielectric constant attains nearly lowest and stable value.

Relation of the multi-core model with FTIR, XRD patterns and dielectric properties

It is experimentally studied that dielectric constant tends to decrease in EB with the increase of nanostructuration. This phenomenon has been interpreted by constrained movement of dipoles in the interface between ZnO nanofiller and surrounding EB polymer matrices. Spherical shape of ZnO in nanometric size as nanofiller, content in polymer matrix, inter filler distances and interfacial morphology play their role for dielectric variation which has been explained on the basis surface defects in ZnO crystal and various interactions of EB chains with ZnO nanoparticle. FTIR studies of the composite shows the presence H-bonding between ZnO nanoparticles and –NH- group of EB resulting in the formation of bonded layer. XRD patterns clearly confirm the dilution of EB peak due to adsorption/interaction between ZnO and EB. Formation of second bound layer has been explained on the basis of defect sites in nanoparticles interaction with the EB chains. Loose layer formation has been explained on the basis of high surface to volume ratio of ZnO nanoparticles. However, further studies are being carried with polypyrrole/polythiophene-metal oxide nanoparticles to prove the concept.

Conclusions

The dielectric behaviour of the EB–ZnO nanocomposites films was found to change drastically in comparison to pure EB in the region 1 kHz–1 MHz with the increase of nanoparticles concentration in the composite. This change in dielectric behaviour is due to the multilayered interface formed between ZnO nanoparticles and EB. The high energy surface of the ZnO nanoparticles leads to the decrease in dielectric constant. TEM and XRD analysis show some enlargement of the ZnO nanoparticles embedded in the EB matrix. FTIR also confirms the attachment of the EB chains with nanoparticles.

References

Andeen D, Lofler L, Padture N, Flange F (2003) Crystal chemistry of epitaxial ZnO on (1 1 1) MgAl$_2$O$_4$ produced by hydrothermal synthesis. Cryst Growth 259:103–109

Bal K, Kothari VK (2009) Mesurement of dielectric properties of textile material and their application. Indian J Fibre Text Res 34:191–199

Cao Y, Smith C, Heeger AJ (1992) Counter-ion induced processibility of conducting polyaniline and of conducting polyblends of polyaniline in bulk polymers. Synth Met 48:91–97

Chen Y, Bangnall DM, Ko H, Hiraga K, Zhu Z, Yao T (1998) Plasma assisted molecular beam epitaxy of ZnO on *c*-plane sapphire: growth and characterization. J Appl Phys 84:3912–3918

Crisler DF, Cupal JJ, Moon AR (1968) Dilectric piezoelectric and electromechanical coupling costants of zinc oxide crystals. Proc Lett IEEE 56:225–226

Dang ZM, Fan LZ, Zhao SJ, Nan CW (2003) Preparation of nanosized ZnO and dielectric properties of composites filled with nanosized ZnO. Mater Sci Eng B 99:386–389

Gangopadhyay R (2000) Conducting polymer nanocomposites: a brief overview. Chem Mater 12:608–622

Hagemark KI (1976) Defect structure of zinc-doped zinc oxide. J Solid State Chem 16:293–299

Harsányi G (1995) Polymer film in sensor application (technology material devices and their characterization). Technomic Publishing Company, Inc., Lanchaster, pp 34, 99

He Y (2005) A novel emulsion route to sub-micrometer polyaniline/nano-ZnO composite fibers. Appl Surf Sci 249:1–6

Huang HC (2010) Preparation and characterization of highly transparent UV-curable ZnO-Acrylic nanocomposites. Cera Int 36:1245–1251

Joseph Mathai C, Saravanan S, Anantharaman MR, Venkitachalam S, Jayalekshmi S (2002) Characterization of low dielectric constant polyaniline thin film synthesized by ac plasma polymerization technique. J Phys D Appl Phys 35:240

Koch MH, Timbrell PY, Lamb RN (1995) The influence of film crystallinity on the coupling efficiency of ZnO optical modulator waveguides. Semicond Sci Technol 10:1523–1527

Liang S, Sheng H, Liu Y, Hio Z, Lu Y, Shen H (2001) ZnO Schottky ultraviolet photodetectors. Cryst Growth 225:110–113

MacDiarmid AG, Epstein AJ (1989) Polyanilines: a novel class of conducting polymers. Faraday Discuss 88:317–332

MacDiarmid AG, Epstein AJ (1994) The concept of secondary doping as applied to polyaniline. Synth Met 65:103–116

Nelson JK, Hu Y (2004) The impact of nanocomposite formulations on electrical voltage endurance. IEEE-ICSD 7:832–835

Ozgur U, Alivov YI, Liu C, Teke A, Reshchikov MA, Dogan S, Avrutin V, Cho S-J, Morkoc H (2005) A comprehensive review of ZnO materials and devices. J Appl Phys 98:041301

Paul GK, Bhaumik A, Patra AS, Bera SK (2007) Enhanced photo-electric response of ZnO/polyaniline layer-by-layer self-assembled films. Mater Chem Phys 106:360–363

Pouget JP, Jozefowicz ME, Epstein AJ, Tang X, MacDiarmid AG (1991) X-ray structure of polyaniline. Macromolecules 41:723–789

Saito N, Haneda H, Sekiguchi T, Ohashi N, Sakaguchi I, Koumoto K (2002) Low-temperature fabrication of light-emitting zinc oxide micropatterns using self-assembled monolayers. Adv Mater 14:418–421

Seow ZLS, Wong ASW, Thavasi V, Jose R, Ramakrishna S, Ho GW (2009) Controlled synthesis and application of ZnO nanoparticles, nanorods and nanospheres in dye sensitized solar cells. Nanotechnology 20:6

Sharma BK, Gupta AK, Khare N, Dhwan SK, Gupta HC (2009) Synthesis and characterization of polyaniline–ZnO composite and its dielectric behavior. Synth Met 159:391–395

Stejskal J (2002) Polyaniline: preparation of a conducting polymer (IUPAC technical report). Pure Appl Chem 74:857–867

Tan Y, Zhang Y, Thavasi V, Kan J (2009) Synthesis and properties on polyaniline in the presence of nickel chloride. eXPRESS Polym Lett 3:336–337

Tanaka T, Kozako M (2005) Proposal of a multi-core model for polymer nanocomposite dielectric. IEEE Trans Dielectr Electr Insul 12:669–681

Zeng XR, Ko TM (1997) Structure-conductivity relationships of iodine-doped polyaniline. J Polym Sci 35:1993–2001